ELSEVIER

Journal of Hazardous Materials B137 (2006) 1025–1034

Journal of Hazardous Materials

www.elsevier.com/locate/jhazmat

Degradation of chemical warfare agent simulants using gas–liquid pulsed streamer discharges

Mayank Sahni, Bruce R. Locke *

Department of Chemical and Biomedical Engineering, Florida State University, FAMU-FSU College of Engineering, 2525 Pottsdamer Street, Tallahassee, FL 32310, USA

Received 29 January 2006; received in revised form 13 March 2006; accepted 15 March 2006
Available online 5 May 2006

Abstract

This study determines the effectiveness of pulsed streamer discharges (PSD), a type of advanced oxidation technology (AOT) to clean water contaminated with chemical agents. For the purpose of this study, experiments were conducted with G and H agent simulants to determine the degradation kinetics and to determine the effects of various electrical and chemical parameters in the degradation of these contaminants. The energy efficiency of contaminant degradation shows that pulsed streamer discharges can be an efficient technology in treating water contaminated with chemical agents. The maximum energy yields of degradation of H and G agent simulants by the pulsed corona discharges are 0.029 and 0.008 molecules/100 eV, respectively, in the series configuration with ferrous sulfate salt in solution.

Keywords: Gas–liquid pulsed streamer discharges; Chemical agent simulants; Hydroxyl radicals

1. Introduction

Stockpiles of various chemical warfare agents (CWA) are an imminent environment threat. Although production of these harmful chemicals is banned and current reserves are to be destroyed in accordance with international treaties, the storage and transportation of these chemicals is a critical concern. Previous experiences have shown that improper handling and storage of hazardous chemicals result in their leaking into the environment through both water and air. New technologies are being considered as alternatives to conventional technologies (incineration and chlorination) to degrade chemical warfare agents [1]. This thrust is attributed to the inability of conventional technologies to degrade the CWA into benign compounds without forming toxic by-products. Conventional methods for water remediation, including carbon adsorption, biological treatment, and chlorine treatment, suffer from various limitations and generally are either not active in destroying the target species or have very slow rates of destruction. Both oxidative and reductive technologies have shown potential in degrading CWA in laboratory testing and certain technologies such as L-Gel and atmospheric pressure plasma jet hold promise for field scale studies [2,3]. The photocatalytic and photolysis degradation of various simulants in the liquid and gas phases have also been investigated in laboratory scale studies and the pathways for the degradation of simulants were predicted based on identification of degradation by-products [4]. The degradation of 2-chloroethyl phenyl sulfide (H agent simulant) on alumina, polyvinylbenzene (impregnated with NaOH, polyethylene glycol, and polyethylenimine), and Amberguard XE-555, the degradation of 2-chloroethyl phenyl sulfide (H agent simulant) and *O*,*S*-diethyl phenylphosphonothioate (VX simulant) on zeolites (NaY and AgY), hydrolysis of *O*,*S*-dialkyl phenylphosphonothioates in alkaline conditions and with *o*-iodosobenzoate (IBA), and the reactions of surfactants such as potassium *O*,*O*′-didodecylphosphorodithioate with H agent simulant (2-chloroethyl phenyl sulfide) have been explored by various researchers [5–8].

This study deals with testing the pulsed streamer discharge (PSD) technology as a means to decontaminate water in the unfortunate circumstance of CWA leaking into water supplies. Pulsed streamer discharges are primarily used in water and gas purification and comprise a broader set of technologies

* Corresponding author. Tel.: +1 850 410 6165; fax: +1 850 410 6150.
E-mail address: locke@eng.fsu.edu (B.R. Locke).

0304-3894/$ – see front matter © 2006 Elsevier B.V. All rights reserved.
doi:10.1016/j.jhazmat.2006.03.029

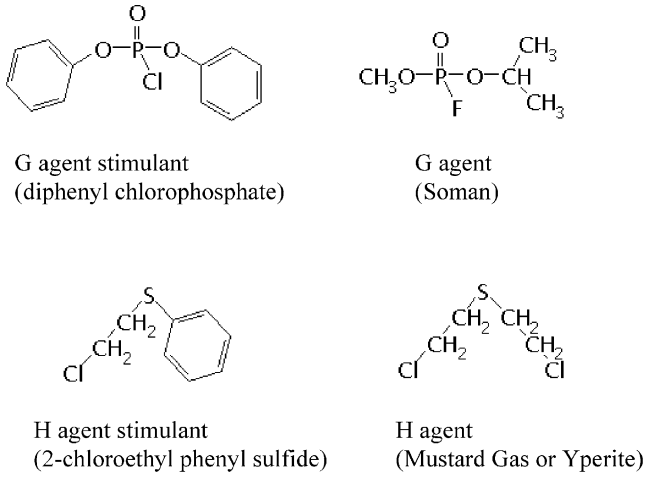

Fig. 1. Structure of the selected stimulant compounds and their analogous chemical agents.

called advanced oxidation technologies (AOT). These technologies are based primarily on production of the hydroxyl radical, a highly oxidative species, but certain technologies such as pulsed streamer discharges also produce other oxidative (H_2O_2, O_3, $O^{\bullet}$, and $HO_2^{\bullet}$) and reductive species ($H^{\bullet}$ and $O_2^{\bullet -}$). The development of PSD technology has resulted in reactor modifications enabling simultaneous generation of discharges in gas and liquid phases using a single power supply. These reactor configurations called the series and parallel configurations have shown a higher rate of degradation of certain organics (phenols, substituted phenols, nitrobenzene, and organic dyes) at a similar energy consumption compared to the conventional purely liquid phase discharge configuration [9–12].

The overall objective of developing pulsed streamer discharges into an effective countermeasure system for the destruction of chemical agents is achieved by performing laboratory scale tests of several prototypes of batch PSD reactors for the destruction of two model chemical compounds 2-chloroethyl phenyl sulfide (CEPS) (H agent simulant) and diphenyl chlorophosphate (DPCP) (G agent simulant). The structures of the simulants and the analogous chemical agents are shown in Fig. 1.

2. Experimental techniques and methods

2.1. Materials

The chemicals used in the present study were used as received from the manufacturer. They include ferrous sulfate, acetonitrile (HPLC grade), trifluoroacetic acid (from Fisher Scientific), 2-phenyl thioethanol (Acros Chemicals), 2-chloroethyl phenyl sulfide, diphenyl chlorophosphate, platinum on 30–150 mesh carbon (all from Aldrich Chemical Company). Deionized water of conductivity less than 1 μS/cm was obtained from a Barnstead deionized water unit (reverse osmosis followed by ion exchange treatment).

2.2. Pulsed generation network

The power supply to generate high voltage pulsed electrical discharges is the same as used previously and has been described in detail in earlier work [13]. It consists of a dc power supply containing rectifiers to provide an ac output voltage. This is half wave rectified by a series of rectifiers and passes through a set of current limiting resistors (333 kΩ) to a bank of capacitors (2000 pF) that stores the charge until a rotating spark gap (60 Hz) aligns with copper electrodes and the charge is diverted to the reactor to initiate an electrical discharge. The copper electrodes are used only inside the spark gap power forming system and not inside the reactor. Nickel chromium needle electrodes are used to deliver the high voltage discharge into the reactor liquid phase for all experiments. The ground electrode for all reactors is made of reticulated vitreous carbon and the same material is used for the high voltage gas phase electrode in the parallel configuration. Approximately 1 J of energy is input into the reactor per pulse and since 60 pulses are initiated each second the total energy input into the reactor is approximately 60 J/s. The applied voltage and current waveforms were recorded for some experiments. A Tektronix P6015A high voltage probe coupled to a Tektronix TDS 460 fast digital storage oscilloscope along with the P6021 Tektronix current probe were used to record the peak voltage, rise time, and pulse width and the reactor electrical power was calculated by importing the data and integrating using Simpson's rule. Typical voltage and current waveforms are shown in Fig. 2.

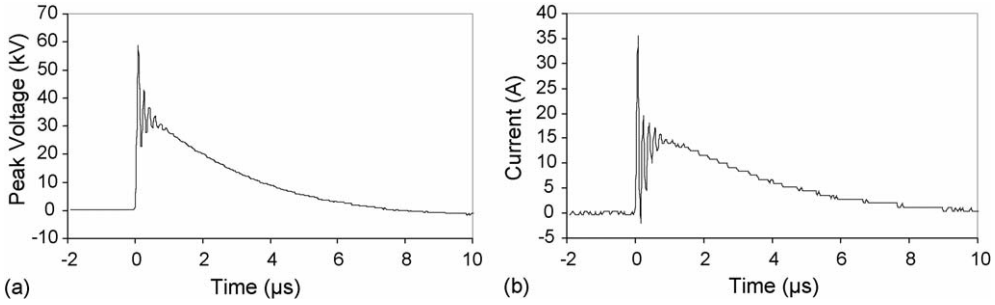

Fig. 2. Typical voltage (a) and current (b) waveforms (applied voltage = 45 kV, initial conductivity = 150 μS/cm, reference configuration).

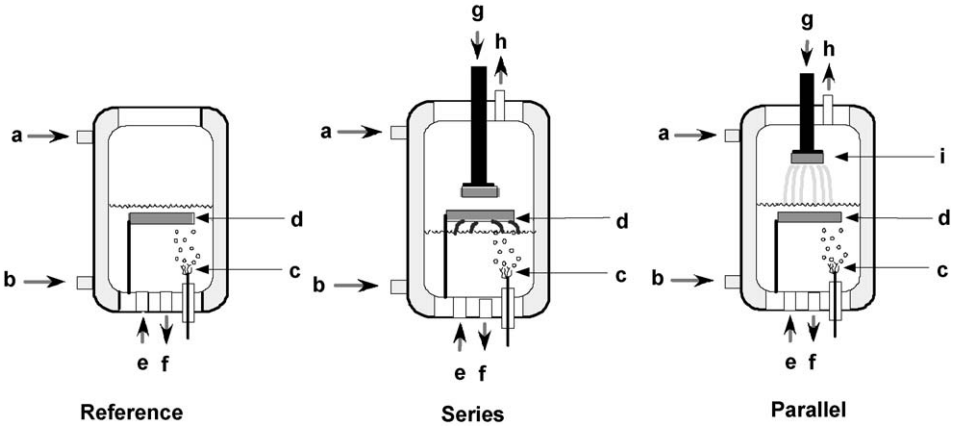

Fig. 3. Schematic view of the different reactor configurations (reference, series, and parallel) ((a and b) cooling water inlet and outlet; (c) liquid phase high voltage electrode; (d) ground electrode; (e and f) recirculation inlet and outlet; (g and h) gas inlet and outlet; (i) gas phase high voltage electrode).

2.3. Reactor configurations

The reactor configurations used in this study have been described before in previous publications and the schematic of the different reactor configurations is shown in Fig. 3 [9,14]. It is important to mention here that insertion of different electrodes through the base and the top (made of Teflon) of the reactor (made of glass) afforded us the advantage of using the same reactor system for the various configurations. In the reference configuration only the liquid phase discharge is produced because both the high voltage electrode and the ground electrode are submerged in the solution. There is no gas flow through the headspace above the solution in this reactor configuration. In the series configuration the ground electrode is placed above the solution level so that discharge forms in both phases. In this case the liquid phase discharge is similar to the reference configuration, but the gas phase discharge consists of intense streamers that are fairly uniformly distributed across the interface between the ground electrode and the water surface [15]. Oxygen at 400 ml/min flows through the reactor in the series case. The gap distance between the ground electrode and the gas–liquid interface is an important parameter in the series configuration; therefore, this distance was kept constant by injecting the same volume of the initial contaminant solution as that of the sample drawn from the reactor. The parallel configuration differs from the other reactors because it features two high voltage electrodes: one each in the liquid and gas phases. The liquid phase discharge is similar to the liquid phase discharge in the other two configurations; however, the gas phase discharge consists of faint streamers resembling the streamers produced in gas phase pulsed streamer experiments [16]. The gas flowing through the reactor headspace is a mixture of argon (200 ml/min) and oxygen (150 ml/min) to ensure a stable gas phase discharge and to maximize the ozone generation in the gas phase discharge [17]. The inlet and outlet fittings in the base of the reactor were attached to 3/8 in. HDPE tubes and a brief section of Tygon tubing to transfer the solution to a peristaltic pump to ensure well-mixed conditions inside the reactor.

The volumes of contaminant solution treated in the reference, series, and parallel configurations are 700, 550, and 650 ml, respectively. All experiments during this study (except some at 60 kV) were conducted at an applied voltage of 45 kV with the stimulant concentration of 100 ppm. Experiments were performed to determine the effect of $FeSO_4$. Solution conductivity and pH were measured before and after pulsed streamer treatment using a handheld meter (OAKTON Instruments, Vernon Hills, IL). Samples of 4 ml volume were drawn regularly during experiments using a three-way valve located between the reactor and pump on the reactor's outlet line. Samples from some experiments were also analyzed by ion chromatography to determine the concentration of chlorides, sulfates, and phosphates in solution.

2.4. Properties of simulants chosen

Due to the extremely toxic nature of chemical warfare agents, laboratory scale studies to determine various chemical and physical characteristics are conducted on simulant compounds that mimic the chemistry of the agents but are considerably less toxic. The simulants chosen for this study have at least one phenyl group that reduces the toxicity of the chemicals considerably. The H agent simulant chosen for this study is 2-chloroethyl phenyl sulfide that is very similar in structure to sulfur mustard (H agent) as shown in Fig. 1. It was found that the CEPS dissolves slowly and hydrolyzes; therefore, the solution was stirred for 48 hours to ensure that the hydrolysis product 2-phenyl thioethanol (2-hydroxyethyl phenyl sulfide (HEPS)) reaches a stable concentration (also confirmed by ion chromatography which shows a stabilization of the chloride ion values (Table 3)). Other researchers have also observed similar behavior where chlorinated H-simulants release the chloride in solution and hydrolyze slowly [4]. The identity of the hydrolysis product of H agent simulant was confirmed by injecting a pure standard of 2-phenyl thioethanol onto the HPLC and comparing the retention time. The solution conductivity after stirring for 48 h was measured (~250 μS/cm) and was sufficient to initiate a discharge in the liquid phase without the addition of any further salts. The G agent simulant (DPCP) also hydrolyzes slowly and therefore the DPCP stock solution was stirred for 48 hours to ensure complete hydrolysis. Although the concentration of the single

Table 1
The solvent profile for analysis and detection of CEPS and its degradation by-products by HPLC

Minutes	Water (%)	Acetonitrile (%)
0–5	90	10
5–14	70	30
14–24	50	50
24–34	20	80

hydrolysis product stabilized in less than 24 hours the solution was stirred for 48 hours to prevent any discrepancy between different solutions (also confirmed by ion chromatography which shows a stabilization of the chloride ion values). Researchers have shown that chlorophosphates hydrolyze by a $S_N2(P)$ mechanism and the products of diphenyl chlorophosphate are ester and acid compounds [18]. The solution conductivity after stirring was measured (~290 μS/cm) and was sufficient to initiate a discharge in the liquid phase without the addition of any further salts.

2.5. Analytical techniques and procedures

The hydrolysis of the chlorinated simulants dictated the use of an analytical technique other than gas chromatography with an electron capture detector that was ineffective due to loss of chlorine atom from the compounds upon hydrolysis. A Perkin-Elmer HPLC and a UV detector were therefore used to detect the hydrolysis product of the CWA simulants and the various degradation by-products. A Supelco Supelcosil LC-18 column (25 cm × 4.6 mm) and Perkin-Elmer's proprietary software Turbochrom were used for separation and quantification. The methods employing gradients in the solvent flow to separate and analyze the stimulant compounds using HPLC were developed by modifying a method developed for H agent by-product analysis on the HPLC by Rainer [19]. For analysis of 2-chloroethyl phenyl sulfide (CEPS), a mobile phase consisting of deionized water and aceonitrile at a flow rate of 2 ml/min was used. The composition of the mobile phase is shown in Table 1. For analysis of diphenyl chlorophosphate hydrolysis and degradation by-products a mobile phase consisting of deionized water containing 0.01% trifluoroacetic acid and aceonitrile at a flow rate of 1 ml/min was used. The composition of the mobile phase is shown in Table 2.

The UV absorbance detector wavelength used for analysis of 2-chloroethyl phenyl sulfide hydrolysis and degradation by-products was 240 nm and for diphenyl chlorophosphate hydrolysis and degradation by-products it was 220 nm. The detection wavelength for detection of both simulants was different from their peak absorbances to prevent the simulant peak from going over the range on the UV detector. Trifluoroacetic acid was added to deionized water in order to produce a sharper peak for the diphenyl chlorophosphate hydrolysis product.

Table 2
The solvent profile for analysis and detection of DPCP and its degradation by-products by HPLC

Minutes	Water with TFA (%)	Acetonitrile (%)
0–2	80	20
2–12	50	50
12–22	20	80

The effect of pH was not studied; however, the pH change for the case of the H agent stimulant solution was not significant. The initial pH was acidic, approximately 3.4, and the final pH of the solution after treatment in the series case was around 3.2. This was typical of all reactor configurations with the series giving the greatest pH change.

3. Results and discussion

Control experiments where the solution of hydrolysis product (HEPS) of H simulant (CEPS) (initial concentration = 5.79×10^{-4} M) was added to the reactor without any pulsed streamer discharge treatment show no loss of the simulant due to adsorption on the reactor surfaces or due to vaporization (Fig. 4). The degradation observed in the reference configuration (purely liquid phase discharge reactor) is nearly 26% after 60 min of PSD treatment. The formation of various oxidative (H_2O_2, $OH^\bullet$, and $HO_2^\bullet$) and reductive ($H^\bullet$) species has been documented in the reference configuration [20–22]. Most of the organic contaminants react with high reaction rate constants with hydroxyl radical produced by the pulsed streamer discharges and their degradation can be accounted for predominantly by hydroxyl radical attack. Using chemical probes the rate of hydroxyl radical production has been estimated at 45 kV (and at 150 μS/cm initial conductivity of solution) and has been found to be dependent on the concentration of probe in solution [23]. Based on experimental evidence it is clear that the reactive species such as hydroxyl and hydrogen radicals that are produced in the discharge have very high local concentrations near the discharge zone in comparison to the contaminants and probe compounds that are present in solution and are distributed uniformly in the bulk of the solution. Therefore, these radical species undergo recombination reactions (to produce molecular species such as hydrogen peroxide and hydrogen) in the discharge zone preferentially over reactions with probes. Unless the

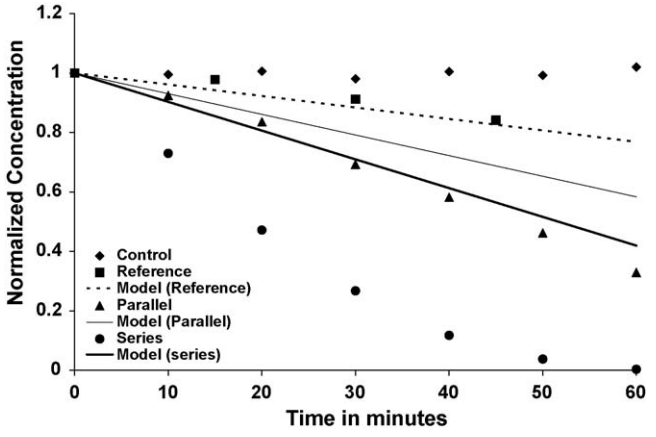

Fig. 4. HEPS degradation for various reactor configurations with no additives in solution (applied voltage = 45 kV, CEPS concentration = 100 ppm, initial conductivity ≅ 250 μS/cm).

concentration of probes is high enough to ensure that they compete with radical recombination reactions the probes will react with the reactive species (primarily hydroxyl radicals) that diffuse into the bulk of the solution. The zero order rate of production of hydroxyl radical at probe (disodium salt of terephthalic acid) concentration of 5×10^{-4} M (that is nearly similar to the concentration of 2-chloroethyl phenyl sulfide (5.79×10^{-4} M) in solution) was determined to be 1.67×10^{-8} M s^{-1} [23].

A batch reaction kinetics model, developed earlier to model phenol degradation by pulsed streamer discharges by Grymonpre et al. [13] that contains three fundamental reactions (having a zero order rate of production of reactive species by the pulsed streamer discharges determined from experiments [21]) and other reactions derived from radiation chemistry literature, was modified for predicting the degradation of hydrolysis product of the H agent simulant (modifications listed in Appendix A). The zero order rate of formation of hydroxyl radicals determined by experiments [23] in the reference configuration was incorporated into the model and it was assumed that the rate constant of reaction of 2-hydroxy phenyl sulfide with hydroxyl radicals is diffusion limited. This assumption was made since the rate constant of several aromatic and sulfide species with hydroxyl radicals is close to diffusion limit (with benzene = 7.8×10^9 M^{-1} s^{-1}; with diethyl sulfide = 1.4×10^{10} M^{-1} s^{-1}) [4]. The degradation of the contaminant after 60 min of PSD treatment at 45 kV predicted by the model is expected to be 23.2% (Fig. 4, dashed line for reference model). The degradation of 2-hydroxyethyl phenyl sulfide observed in the PSD experiments in the reference configuration is similar to that predicted by the batch kinetics model that simulates the reference configuration. This implies that if hydroxyl radical attack is the primary degradation mechanism of the 2-hydroxyethyl phenyl sulfide the rate constant of the reaction of hydroxyl radicals and 2-hydroxyethyl phenyl sulfide is nearly 1×10^{10} M^{-1} s^{-1}.

Experiments in the three different reactor configurations show that the hybrid configurations perform considerably better than the reference configuration with the hybrid-series degrading the HEPS (CEPS initial concentration = 5.79×10^{-4} M) completely in less than 60 min of discharge. Earlier work has shown that the hydrogen peroxide production in the liquid phase is quantitatively similar in the three different reactor configurations while the production rate of ozone in the gas phase of the series and parallel configurations has been quantified to be around 20 and 120 mg/h, respectively [9]. However, the advantage of hybrid reactors is not just in ozone generation, the additional discharge in the gas phase and on the gas–liquid interface can produce short- and long-term reactive species that dissolve in water to degrade contaminants. The intense discharge at the gas–liquid interface in the series configuration has been shown to contribute substantially more hydroxyl radicals to the solution [24]. Although the discharge in the gas phase of the parallel configuration consists of faint streamers that visually propagate from the gas phase high voltage electrode towards the wall of the reactor, the ground electrode is submerged in the solution and therefore reactive species such as hydroxyl radicals are also produced in the liquid phase due to this discharge. This leads to a higher hydroxyl radical production in the parallel configuration and this was confirmed by performing experiments with hydroxyl radical probe disodium salt of terephthalic acid (NaTA) [24].

The model and experimental data comparison of degradation of 2-hydroxyethyl phenyl sulfide is rather poor for hybrid reactor configurations with the experimentally observed degradation being much greater than model predictions (Fig. 4, solid lines for series and parallel models). The model for the hybrid reactor configurations incorporates the zero order hydroxyl radical production rates determined from experiments with hydroxyl radical probe NaTA in the series and parallel configurations. The discrepancy between the model–experimental data observed in the case of the hybrid reactors suggests that there is a reactive species other than hydroxyl radical produced by the hybrid reactors (and not the reference configuration) that causes a substantial component of the HEPS degradation. Based on our current knowledge about hybrid reactors, ozone is the only reactive species that is produced in the hybrid configurations and that is absent in the reference configuration. Researchers have shown that the ozone generated in the gas phase of the hybrid configurations can subsequently dissolve into the solution and react with contaminants present in the solution. Experiments with phenol in the hybrid-series configuration have resulted in formation of *cis*,*cis*-muconic acid, a by-product characteristic of direct ozone attack on phenol [10]. The reactivity of the CEPS or HEPS with ozone is not known but it is conceivable that the ozone molecule can attack the aromatic ring of the compound. Higher production of ozone in the gas phase has been reported in the parallel configuration (∼3000 ppm) as compared to the series configuration (∼350 ppm) but experiments with RB-137 dye have shown that the transfer of ozone from the gas to the liquid phase is mass transfer limited in the parallel configuration (data not shown). If ozone causes the enhanced degradation observed in the hybrid configuration the mass transfer limitation of ozone can explain why a lower HEPS degradation is observed in the parallel reactor even though the ozone generated in the gas phase is higher as compared to the series configuration.

Previous work has demonstrated the increased efficiency of degradation of contaminants upon using iron salts in solution due to the Fenton's reaction (a series of reactions (1)–(8) that yield hydroxyl radicals from reactions of hydrogen peroxide with iron ions) [13,25,26].

$$Fe^{2+} + H_2O_2 \rightarrow Fe^{3+} + OH^- + {}^{\bullet}OH \quad (1)$$

$$Fe^{3+} + H_2O_2 \rightarrow Fe^{2+} + HO_2^{\bullet} + H^+ \quad (2)$$

$${}^{\bullet}OH + Fe^{2+} \rightarrow Fe^{3+} + OH^- \quad (3)$$

$$Fe^{3+} + HO_2^{\bullet} \rightarrow Fe^{2+} + O_2 + H^+ \quad (4)$$

$$Fe^{2+} + HO_2^{\bullet} \rightarrow Fe^{3+} + H_2O_2 \quad (5)$$

$$Fe^{3+} + O_2^{\bullet -} \rightarrow Fe^{2+} + O_2 \quad (6)$$

$$Fe^{2+} + O_2^{\bullet -} \rightarrow Fe^{3+} + H_2O_2 \quad (7)$$

$$H^{\bullet} + Fe^{3+} \rightarrow Fe^{2+} + H^+ \quad (8)$$

For phenol the concentration of ferrous sulfate was optimized to yield the greatest degradation at 485 μM [13]. The same

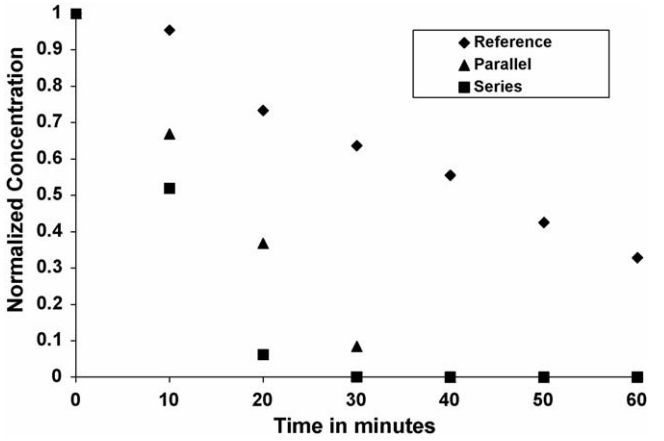

Fig. 5. HEPS degradation for various reactor configurations with 485 μM ferrous sulfate in solution (applied voltage = 45 kV, CEPS concentration = 100 ppm, initial conductivity ≅ 350 μS/cm).

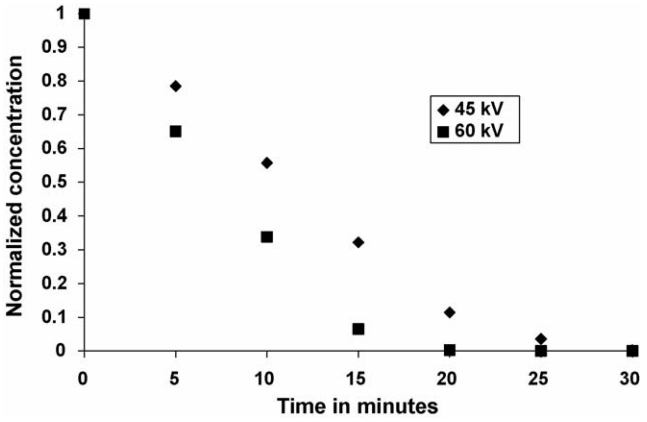

Fig. 6. HEPS degradation in series configuration with 485 μM ferrous sulfate in solution (CEPS concentration = 100 ppm, applied voltage = 45 and 60 kV, initial conductivity ≅ 350 μS/cm).

concentration of ferrous sulfate was used in the present experiments. These experiments show increased degradation due to the Fenton's reactions in comparison to the experiments with no additives in all the reactor configurations (Fig. 5). The rate of degradation in the reference configuration increases from 6.33×10^{-5} to 1.896×10^{-4} M s^{-1}. An important consideration from these results is that although the Fenton's reactions increase the degradation rate of the HEPS, the increase is not as significant as that observed for phenol by previous researchers even though the HEPS experiments were conducted at a pH of around 3 that is known to enhance Fenton's reactions [27]. Two factors can contribute to this result: conductivity of solution and the absence of Fe^{2+} regeneration. Due to hydrolysis of the H agent simulant that leads to release of chloride ions, the initial conductivity of the solution is around 250 μS/cm and upon addition of ferrous salts it increases to nearly 350 μS/cm. Using actinometry experiments the increase of UV component of the solution with increasing solution conductivity has been documented [28]. This is a factor in the decrease of hydrogen peroxide production rate as the conductivity of the solution increases from 150 to 600 μS/cm [27]. The production rate of hydrogen peroxide at an applied voltage of 45 kV (peak voltage = 57 kV) was 8×10^{-7} M s^{-1} at an initial conductivity of 150 μS/cm but decreases to 5×10^{-7} M s^{-1} at an initial conductivity of 300 μS/cm. This results in lower hydrogen peroxide concentration in solution, thereby lowering the rate of generation of hydroxyl radicals due to Fenton's reactions. Another possible reason for the lower rate of formation of hydroxyl radicals from Fenton's reaction in the present experiments could be the absence of a pathway for the regeneration of Fe^{2+} such as that occurring in phenol experiments due to the formation of the intermediate products hydroquinone and catechol [29]. The batch reaction kinetics model developed by Grymonpre shows that in the absence of phenol the Fe^{2+} reacts irreversibly with hydrogen peroxide and is consumed within 15 min; however, with 100 ppm phenol in solution Fe^{2+} ions are regenerated by reactions of hydroquinone and catechol with Fe^{3+} ions [27]. This regeneration step might be missing in degradation of HEPS; therefore, the Fenton's reactions are not as effective as in the case of phenol.

The hybrid reactors also lead to faster degradation of HEPS in the Fenton's case with the hybrid-series reactor providing the fastest degradation (Fig. 6). The hybrid reactors offer considerable improvement in degradation of HEPS compared to the reference configuration in both the no additive and Fenton's experiments. This implies that the gas phase and gas–liquid discharges contribute substantial amounts of reactive species in the solution.

Ion chromatography data corroborate the data obtained by HPLC analysis (Table 3). The chloride concentration for all the H agent simulant experiments shows consistent concentrations in all the experiments (except the no additive series case) and it does not change appreciably during the experiments. This result confirms that the H agent simulant has hydrolyzed to give stable concentrations of the hydrolysis product and that during the experiments additional hydrolysis is very low. For the H agent the change in sulfate concentration during the experiment depends upon the configuration of the reactor. The sulfate

Table 3
Ion chromatography data showing chloride and sulfate concentrations for H agent simulant in various reactor configurations

Before PSD treatment		After 60 min of PSD treatment	
Cl^-	SO_4^{2-}	Cl^-	SO_4^{2-}
Control			
26.28	0.12	26.08	0.11
No additive, reference			
25.56	0.12	26.42	2.53
No additive, series			
15.10	0.11	15.21	5.79
		After 50 min of PSD treatment	
No additive, parallel			
27.71	0.12	27.06	1.81
		After 40 min of PSD treatment	
Fenton's series			
23.77	15.49	26.45	20.12

Table 4
Energy yields for HEPS degradation in different reactor configurations (applied voltage = 45 kV, CEPS concentration = 100 ppm) (treated volumes in the reference, series, and parallel configurations are 700, 550, and 650 ml, respectively)

Configuration (treated volume)	No additive		Fenton's	
	g/kWh	Molecules/100 eV	g/kWh	Molecules/100 eV
Reference (700 ml)	0.275	0.005	0.712	0.012
Series (550 ml)	0.833	0.014	1.660	0.029
Parallel (650 ml)	0.661	0.011	1.480	0.026

concentration in solution indicates the extent of carbon–sulfur bond breakage (Table 3). If 100% of the carbon–sulfur bond breaks a sulfate concentration of 18.53 ppm will be observed in solution. However, the concentration of sulfate in all the reactor configurations is substantially lower indicating that not all the carbon–sulfur bonds have been destroyed. This also implies that the TOC removal is extremely low for the CEPS since TOC removal will also entail significant breakage of the carbon–sulfur bond (although some of the volatile products observed in the photocatalytic degradation of PEHES contain the CS bond their concentration is not expected to be high [4]).

The energy yields of treating the H agent simulant in the various reactor configurations based on the conversion of the primary contaminant 2-hydroxyethyl phenyl sulfide into intermediate products are expressed in terms of two commonly used units in advanced oxidation literature, grams of contaminant degraded per kilowatt hour of energy consumption, and molecules of contaminant degraded per 100 eV of energy consumption (Table 4). Estimates of energy yields made on the basis of the experimental results show that the pulsed streamer discharge treatment degrades the H agent stimulant in all the reactor configurations with the series configuration providing the highest energy yield (1.660 g/kWh) followed by the parallel (1.480 g/kWh) and reference configurations (0.712 g/kWh), respectively. The photolytic degradation of the H simulant 2-phenylethyl-2-chloroethyl sulfide was found to be 0.06 g/kWh in experimental conditions similar to the present study [4]. The authors hydrolyzed the H agent simulant and started irradiation after stabilization of the total organic carbon (TOC) and chloride content of the solution. The degradation was reported in terms of lowering of total organic carbon content of the solution. Although the energy yield of the H agent degradation observed in PSD treatment is considerably higher than the photolytic degradation, ion chromatography data show that TOC removal for all the reactor configurations is very low. Therefore, the energy yield of PSD degradation reported in terms of TOC removal is expected to be considerably lower. Based on initial experimental results pulsed streamer discharges represent a feasible alternative to the other advanced oxidation technologies currently being investigated for chemical warfare agent degradation. A problem observed during photocatalytic degradation of CWA simulants that could lead to higher cost and can be avoided using PSD technology is the cost of photocatalyst replacement since the adsorption of reaction products leads to photocatalyst deactivation [4].

The commonly observed by-products of H simulants are sulfones and sulfoxides. Vorontsov et al. have predicted several volatile and non-volatile by-products of photocatalytic treatment of an H agent simulant using TMS derivatization and GC–MS detection [4]. The relative concentrations of the by-products were not provided by the authors, but most of the compounds have acidic and alcohol functional groups, thereby giving the compounds sufficient polarity. Photocatalytic degradation of 2-phenylethyl-2-hydroxyethyl sulfide (PEHES), the hydrolysis product of 2-phenylethyl-2-chloroethyl sulfide (PECES), leads to several volatile by-products such as styrene, benzaldehyde, and benzalacetaldehyde. Conceivably similar reaction products are also formed from the degradation of 2-hydroxyethyl phenyl sulfide by pulsed streamer discharges. The quantum efficiency of H agent degradation in the gas phase by photocatalysis has been found to be orders of magnitude higher than liquid phase photocatalysis and the rapid mineralization was observed in the gas phase [4]. Therefore, treating H agent simulants with hybrid reactors has greater importance because it is likely that the volatile by-products of H agent simulant degradation in the liquid phase are degraded to products such as CO_2 quite rapidly after being subjected to gas-phase discharge in the hybrid configurations. The non-volatile products of PECES and PEHES photocatalysis include phenylethanethiol-2,2-phenylsulfinic acid, benzeneaceticacid, and benzoic acid among others. Based on the products formed the mechanism of PEHES photocatalytic degradation has been proposed to be hydroxyl radical attack that leads to C–S bond cleavage to form thiols and alkenes. Similar products are also expected in PSD treatment since an important mode of 2-hydroxyethyl phenyl sulfide degradation is hydroxyl radical attack. In the present study, the HPLC analysis of the by-products resulting from 2-hydroxyethyl phenyl sulfide shows that some of the by-products are more polar than the H agent simulant itself since they elute earlier from the reverse phase column. However, the identity of the by-products has not been determined.

Experiments were also conducted with the G agent simulant (diphenyl chlorophosphate). The diphenyl chlorophosphate results show similar trends as the H agent simulant where the series reactor configuration yields the highest degradation. Experiments with the G agent stimulant (3.72×10^{-4} M) in the no additives cases show that nearly 34 and 75% of the primary contaminant (hydrolysis product of the DPCP) is removed in the reference and series configurations, respectively, as shown in Fig. 7. The degradation rate of the hydrolysis product of DPCP, however, is faster than HEPS degradation rate in the reference configuration but slower in the series configuration. The batch reaction kinetics model was also modified for predicting the degradation of G agent simulant degradation by pulsed streamer discharges. Since the rate constant of the primary hydrolysis product of the G agent with hydroxyl radicals was not known the rate constant was varied until the degradation predicted by the model was similar to the experimentally observed degradation. The rate constant of reaction obtained this way is $5 \times 10^9\ M^{-1}\ s^{-1}$. The reaction rate constants with hydroxyl radicals of simulants similar to DPCP (dimethyl methylphosphonate (DMMP) and diethyl methylphosphonate (DEMP)) have

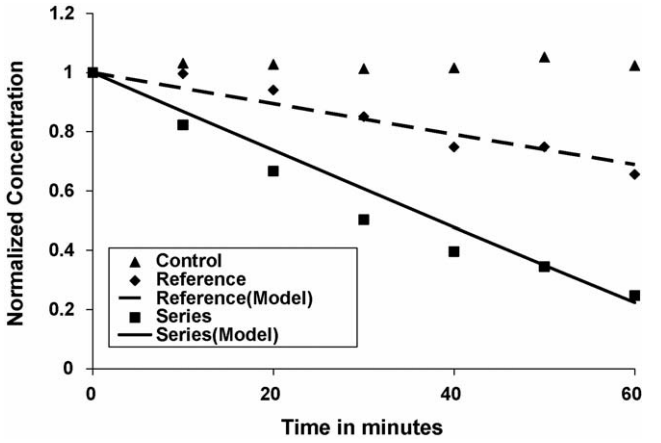

Fig. 7. Degradation of G agent simulant in various reactor configurations with no additives added to solution (DPCP concentration = 100 ppm, applied voltage = 45 kV, initial conductivity ≅ 290 μS/cm).

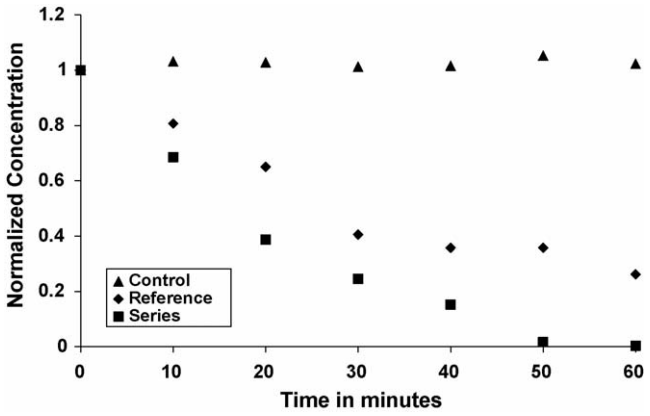

Fig. 8. Degradation of G agent simulant in various reactor configurations with 485 μM ferrous sulfate added to solution (DPCP concentration = 100 ppm, applied voltage = 45 kV, initial conductivity ≅ 400 μS/cm).

been determined by Aguila et al. [30]. The authors determined that DEMP reacts faster with hydroxyl radicals with a reaction rate constant of $6 \times 10^8\ M^{-1}\ s^{-1}$ while that of DMMP is $2 \times 10^8\ M^{-1}\ s^{-1}$. They also observed no reaction of DMMP and DEMP with hydrated electrons and superoxide radical ions in pulse radiolysis and γ-irradiation studies. Since DPCP has two phenyl rings the reactivity with hydroxyl radicals is expected to be greater than DEMP; therefore, the value obtained from the model appears reasonable. This rate constant of reaction was input into the model to predict the degradation of the DPCP hydrolysis product in the series configuration. The experimental and the model predicted degradation is quite similar indicating that the degradation of the hydrolysis product of DPCP in the series configuration is dominated by hydroxyl radical attack. This can also explain the higher degradation of the H agent simulant in the series configuration as compared to the G agent stimulant. Since the H agent simulant reacts with ozone and possibly other reactive species (apart from hydroxyl radicals) produced by the gas and gas–liquid discharge in the series configuration the degradation of the H agent simulant is enhanced; however, the G agent simulant reacts primarily with hydroxyl radicals; therefore, no such enhancement is observed. Experiments with the hydrolysis product of DPCP with ferrous sulfate in solution show an increase of degradation of the contaminant due to Fenton's reactions (Fig. 8). With ferrous salts in solution the series configuration leads to considerably faster degradation in comparison to the reference configuration proving that hydroxyl radicals produced by Fenton's reactions are not the only reactive species in the hybrid reactor configurations.

The HPLC analysis of G agent simulant (DPCP) degradation yields at least four distinct by-product peaks. All the by-product peaks elute (2.10, 4.1, 5.7, and 6.7 min) before the peak of the hydrolysis product of diphenyl chlorophosphate (7.30 min). The earlier elution signifies that all the by-products are more polar than the G agent simulant. The two by-products that elute the earliest increase in concentration throughout the course of the experiments, while the later two by-products increase to a maximum and then decrease for the series configuration with ferrous sulfate added to solution (best case degradation). The ion chromatography data for the DPCP experiments show that the chloride concentration maintains a stable value during the course of the experiments (Table 5). The variability in the initial chlorine as well as the difference in chlorine content before and after the experiments is greater for these experiments than in the CEPS experiments. The maximum phosphate concentration in the DPCP experiments (∼5 ppm) corresponds to nearly 50% of the theoretical maximum that corresponds to complete bond breakage (11.54 ppm) (Table 5).

Table 5
Ion chromatography data showing chloride, and phosphate concentrations for G agent simulant in various reactor configurations

Before PSD treatment		After 60 min of PSD treatment	
Cl^-	PO_4^{3-}	Cl^-	PO_4^{3-}
No additive, reference			
14.94	0	16.11	5.09
No additive, series			
16.38	0	17.27	4.76

The energy yields for DPCP hydrolysis and degradation are shown in Table 6. The energy yields of the DPCP and CEPS degradation show that the hybrid reactors particularly the series reactor configuration provide the highest energy efficiency of degradation. The energy yields of DPCP and CEPS can, however, be improved by optimizing the reactor conditions. The hybrid reactors are sensitive to various electrical, physical, and chemical parameters, e.g. gap distance between the ground

Table 6
Energy yields for DPCP degradation in different reactor configurations (applied voltage = 45 kV, DPCP concentration = 100 ppm)

Configuration (treated volume)	No additive		Fenton's	
	g/kWh	Molecules/100 eV	g/kWh	Molecules/100 eV
Reference (700 ml)	0.365	0.004	0.739	0.007
Series (550 ml)	0.628	0.006	0.830	0.008

electrode and the gas–liquid interface in the series reactor configuration, and these parameters can be experimentally optimized to select the conditions resulting in maximized degradation.

4. Conclusions

Complete degradation of the product of CEPS hydrolysis (HEPS) is observed within 60 min of subjecting it to PSD treatment in the series reactor without additives, and when ferrous sulfate salts are added the degradation is faster (complete removal in 30 min). Ion chromatography showed about 30% of the sulfur bonds are broken, and HPLC showed several by-products of higher polarity than the parent compound increasing with time. The specific energy yields for H agent simulant compound destruction were 0.275, 0.833, and 0.661 g/kWh in the reference, parallel, and series reactors, respectively, without additives. With the addition of iron salts, the specific energy yield increased to 0.712, 1.660, and 1.480, respectively, for the same cases. Although exact comparison with other methods is not possible because of the lack of published results with comparable measures, the removal of total organic carbon by photolysis was reported to be 0.0567 g/kWh. The comparison of the H agent simulant experimental data with the degradation of the H agent stimulant from the existing mathematical model of the reactions occurring in the liquid phase reference pulsed streamer discharge reactor indicates good model–data comparison. This implies that if hydroxyl radicals attack is the primary H simulant degradation mechanism in the reference configuration without any additives in solution the rate of this reaction is close to the diffusion limit in water. Degradation of the H agent simulant in the hybrid reactor cannot be explained by hydroxyl radical attack alone which is highlighted by the discrepancy in the experimentally observed and model obtained degradation. Further work needs to be performed to analyze the by-products of H agent simulant degradation in the various reactor configurations to determine the degradation pathways and relative importance of various reactive species.

The primary product of G agent simulant hydrolysis degrades 75% after subjecting it to 60 min of PSD treatment in the series reactor. The degradation rate increases substantially upon the addition of iron salts to the reference reactor (complete degradation is observed in less than 50 min). Ion chromatography indicated that 50% of the phosphorous was released as phosphate into solution. The specific energy yields for degradation of DPCP were 0.365 and 0.628 g/kWh in the reference and series reactors without additives. In the case with iron salts the yields increased to 0.739 and 0.830 g/kWh. The model incorporating only hydroxyl radical attack of DPCP correctly predicts the experimentally observed degradation of the DPCP in the reference and series configurations. This implies that the degradation of the DPCP occurs primarily by hydroxyl radical attack in both the reference and series configurations.

Acknowledgements

This project was supported by the US Army Corps of Engineers through a SBIR Grant with JCM, Environmental (now Vesitech) of Houghton, MI. Support from FSU for a University Fellowship for MS is also appreciated.

Appendix A

The following changes were made to the reaction developed by Grymonpre et al. [13]:

(1) Reaction (2) of the model was replaced by the reaction:

$$6H_2O \rightarrow 4H_2 + 2H_2O_2 + O_2$$

(2) The zero order rate constant of production of $OH^\bullet$ (reaction (1)) was changed from $9.25 \times 10^{-10}\,M\,s^{-1}$ to reflect the rate constant obtained from hydroxyl radical quantification experiments using NaTA as probe ($1.67 \times 10^{-8}\,M\,s^{-1}$).

(3) The rate constant of production of $OH^\bullet$ (reaction (1)) was altered to reflect the production rate of different reactor configurations and to incorporate the different volumes of solution treated in the three different reactor configurations (reference, hybrid-series, and hybrid-parallel).

(4) The rate constant of production of $OH^\bullet$ (reaction (1)) and H_2O_2 (reaction (2)) was altered to reflect the different initial conductivity of solutions in the no additive and Fenton's cases.

(5) This reaction was included in the model:

$$H_2O \rightarrow H^+ + OH^-, \quad k = 2.52 \times 10^{-5}\,s^{-1}$$

(6) The reaction of HEPS with hydroxyl radicals was included in the model:

$$HEPS + OH^\bullet \rightarrow \text{products}, \quad k = 1 \times 10^{10}\,M^{-1}s^{-1}$$

References

[1] G.W. Wagner, Y.C. Yang, Rapid nucleophilic/oxidative decontamination of chemical warfare agents, Ind. Eng. Chem. Res. 41 (2002) 1925–1928.
[2] E. Raber, R. McGuire, Oxidative decontamination of chemical and biological warfare agents using L-Gel, J. Hazard. Mater. B93 (2002) 339–352.
[3] H.W. Herrmann, I. Henis, J. Park, G.S. Selwyn, Decontamination of chemical and biological warfare agents using an atmospheric pressure plasma jet, Phys. Plasma 6 (1999) 2284–2289.
[4] A.V. Vorontsov, A.D. Davydov, E.P. Reddy, C. Lion, E.N. Savinov, P.G. Smirniotis, Routes of photocatalytic destruction of chemical warfare agent simulants, New J. Chem. 26 (2002) 732–744.
[5] G.W. Wagner, P.W. Bartram, Reactions of VX, HD, and their simulants with NaY and AgY zeolites. Desulfurization of VX on AgY, Langmuir 15 (1999) 8113–8118.
[6] G.W. Wagner, P.W. Bartram, Reactions of the mustard simulant 2-chloroethyl phenyl sulfide with self-decontaminating sorbents. A ^{13}C MAS NMR study, J. Mol. Catal. A: Chem. 111 (1996) 175–180.
[7] F.J. Berg, R.A. Moss, Y.-C. Yang, H. Zhang, Cleavage of phenylphosponothioates by hydroxide ion and by micellar iodosobenzoate, Langmuir 11 (1995) 411–413.
[8] D.A. Jaeger, C.L.I. Schilling, A.K. Zelinin, B. Li, E. Kubicz-Loring, Reaction of a vesicular functionalized surfactant with 2-chloroethyl phenyl sulfide, a mustard simulant, Langmuir 15 (1999) 7180–7185.

[9] P. Lukes, A. Appleton, B.R. Locke, Hydrogen peroxide and ozone formation in hybrid gas–liquid electrical discharge reactors, IEEE Trans. Ind. Appl. 40 (2004) 60–67.
[10] P. Lukes, B.R. Locke, Degradation of substituted phenols in hybrid gas–liquid electrical discharge reactor, Ind. Eng. Chem. Res. 44 (2004) 2921–2930.
[11] A.T. Appleton, P Lukes, W.C. Finney, B.R. Locke, Study of the effectiveness of different hybrid pulsed corona discharge reactors in degrading aqueous pollutants, in: HAKONE VIII, 8th International Symposium on High Pressure, Low Temperature Plasma Chemistry, Puhajarve, Estonia, 2002.
[12] H. Kusic, N. Koprivanac, I. Peternel, B.R. Locke, Hybrid gas/liquid electrical discharge reactors with zeolites for colored wastewater degradation, J. Adv. Oxid. Technol. 8 (2005) 172–181.
[13] D.R. Grymonpre, A.K. Sharma, W.C. Finney, B.R. Locke, The role of Fenton's reaction in liquid phase pulsed corona reactors, Chem. Eng. J. 82 (2001) 189–207.
[14] H. Kusic, N. Koprivanac, B.R. Locke, Decomposition of phenol by hybrid gas/liquid electrical discharge reactors with zeolite catalysts, J. Hazard. Mater. B125 (2005) 190–200.
[15] D.R. Grymonpre, W.C. Finney, R.J. Clark, B.R. Locke, Hybrid gas–liquid electrical discharge reactors for organic compound degradation, Ind. Eng. Chem. Res. 43 (2004) 1975–1989.
[16] M. Kirkpatrick, W.C. Finney, B.R. Locke, Reticulated vitreous carbon electrodes for gas phase pulsed corona reactors, IEEE Trans. Ind. Appl. 36 (2000) 500–509.
[17] T.J. Manning, Production of ozone in an electrical discharge using inert gases as catalysts, Ozone Sci. Eng. 22 (2000) 53–64.
[18] T.W. Bentley, D. Ebdon, G. Llewellyn, M.H. Abduljaber, B. Miller, D.N. Kevill, Chlorophosphate solvolyses evaluation of third order rate laws and rate product correlations for diphenylphosphorochloridate in aqueous alcohols, J. Chem. Soc., Dalton Trans. (1997) 3819–3826.
[19] R. Haas, T.C. Schmidt, Analysis of byproducts of sulfur mustard, UWSF-Z. Umwelchem. Oekotox 8 (1996) 241–242.
[20] P. Sunka, V. Babicky, M. Clupek, P. Lukes, M. Simek, J. Schmidt, M. Cernak, Generation of chemically active species by electrical discharges in water, Plasma Sources Sci. Technol. 8 (1999) 258–265.
[21] A.A. Joshi, B.R. Locke, P. Arce, W.C. Finney, Formation of hydroxyl radicals, hydrogen peroxide and aqueous electrons by pulsed streamer corona discharge in aqueous solution, J. Hazard. Mater. 41 (1995) 3–30.
[22] M. Kirkpatrick, B.R. Locke, Hydrogen, oxygen, and hydrogen peroxide formation in electrohydraulic discharge, Ind. Eng. Chem. Res. 44 (2005) 4243–4248.
[23] M. Sahni, B.R. Locke, Quantification of hydroxyl radicals produced in aqueous phase pulsed electrical discharge reactors, Ind. Eng. Chem. Res., submitted for publication.
[24] M. Sahni, B.R. Locke, The effect of reaction conditions on hydroxyl radical production in gas–liquid pulsed electrical discharge reactors, Plasma Proc. Polym., submitted for publication.
[25] J.J. Pignatello, Dark and photoassisted Fe^{3+}-catalyzed degradation of chlorophenoxy herbicides by hydrogen peroxide, Environ. Sci. Technol. 26 (1992) 944–951.
[26] J.J. Pignatello, K. Baehr, Ferric complexes as catalysts for "Fenton" degradation of 2,4-D and metolachlor in soil, J. Environ. Qual. 23 (1994) 365–370.
[27] D.R. Grymonpre, An experimental and theoretical analysis of phenol degradation by pulsed corona discharge, Ph.D. Thesis, Florida State University, Tallahassee, Florida, 2001.
[28] P. Lukes, Water treatment by pulsed streamer corona discharge, Ph.D. Thesis, Institute of Chemical Technology, Prague, Czech Republic, 2001.
[29] R. Chen, J.J. Pignatello, Role of quinone intermediates as electron shuttles in Fenton and photoassisted Fenton oxidations of aromatic compounds, Environ. Sci. Technol. 31 (1997) 2399–2406.
[30] A. Aguila, K.E. O-Shea, T. Tobien, K.-D. Asmus, Reactions of hydroxyl radical with dimethyl methylphosphonate and diethyl methylphosphonate. A fundamental mechanistic study, J. Phys. Chem. A 105 (2001) 7834–7839.